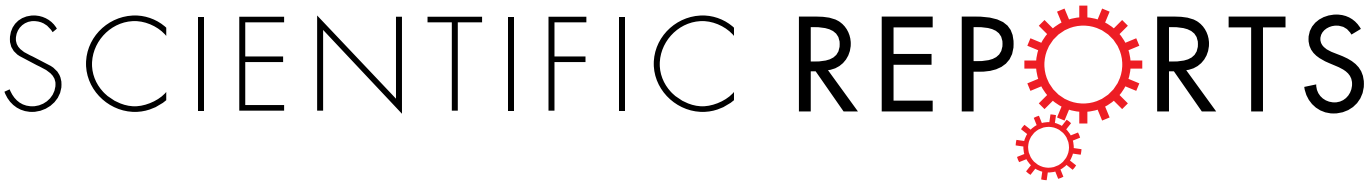

OPEN

Anti-fibrotic impact of Carvedilol in a CCl-4 model of liver fibrosis via serum microRNA-200a/SMAD7 enhancement to bridle TGF-β1/EMT track

Received: 1 May 2018
Accepted: 30 August 2018
Published online: 25 September 2018

Sara A. El-Wakeel[1], Rania M. Rahmo[1] & Hanan S. El-Abhar[2]

Circulating microRNAs (miRNAs) play a role in modulating the prevalence of fibrosis and have been a target of the cardiac anti-fibrotic effect of Carvedilol. However, the impact of miRNAs on the hepatoprotective effect of this non-selective β-blocker has not been yet elucidated. Hence, the current goal is to evaluate the potential role of circulating miR-200a in the hepatic anti-fibrotic pathway of Carvedilol. Male Wistar rats were randomized into normal, CCl_4 (2 ml/kg, i.p, twice weekly for 8 weeks), and CCl_4 + Carvedilol (10 mg/kg, p.o, daily). Carvedilol over-expressed the circulating miR-200a to modulate epithelial mesenchymal transition (EMT) markers (vimentin, E-Cadherin). In turn, Carvedilol increased SMAD7 gene expression and protein content to attenuate the pro-fibrogenic marker transforming growth factor β1 (TGF-β1) and the inflammatory markers (p-38 MAPK and *p*-S536-NF-κB p65). The anti-fibrotic potential was reflected on the decreased expression of the mesenchymal product and EMT marker α-SMA, besides the improved histopathological examination, and the fibrosis scores/collagen quantification to enhance liver functions (AST, ALT, ALP, and AST/platelet ratio index; APRI). In conclusion, circulating miR-200a/SMAD7/TGF-β1/EMT/MAPK axis is crucial in the hepatic anti-fibrotic mechanism of Carvedilol.

Hepatic fibrosis is a process defined by the distortion of hepatic parenchymal cells and their replacement by extracellular matrix or scar[1]. This process is reversible, however, in case of chronic damage it may progress to cirrhosis, a stage that may end up by hepatocellular carcinoma[2]. Hepatotoxins are among the common etiologies highlighting liver fibrosis, such as carbon tetrachloride (CCl_4), which provokes liver injury that reaches fibrosis or cirrhosis according to the duration of damage[3]. Activation of hepatic stellate cells (HSCs) and their acquisition of a myofibroblastic phenotype expressing alpha smooth muscle actin (α-SMA), is a well-established event in the pathogenesis of liver fibrosis[4]. However, recent evidence implicated that epithelial mesenchymal transition (EMT), a process in which epithelial cells acquire a gradual loss of their epithelial phenotype and gain the characteristics of mesenchymal cells, is critical in liver fibrosis pathology, as well. Therefore, fibroblasts were found to be produced from epithelial cells through EMT and not only from HSCs[5]. EMT process involves the loss of the epithelial cell adhesion molecules, like E-Cadherin and Zona occludens (Zo-1) and their substitution with the mesenchymal markers: vimentin, fibronectin, collagen and matrix metalloproteinases (MMP-2 and MMP-9)[6,7].

MicroRNAs (miRNAs) are endogenous small (20–25) nucleotides non-coding RNAs targeting messenger RNA in the cytoplasm and leading to the inhibition of their transfer and translation, hence regulating protein expression involved in fibrosis, inflammation, and oncogenesis. Alteration of circulating miR200a in the serum reveals pathological conditions of the liver and may function as a non-invasive diagnostic marker in progressive liver diseases[8]. It has been reported that miR200 family regulates transforming growth factor (TGF-β1)-induced renal tubular EMT through the SMAD pathway[9]. SMADs are a family of proteins that modulate the fibrogenic

[1]Department of Pharmacology & Toxicology, Faculty of Pharmacy, Misr International University, Cairo, Egypt. [2]Department of Pharmacology & Toxicology, Faculty of Pharmacy, Cairo University, Cairo, Egypt. Correspondence and requests for materials should be addressed to H.S.E.-A. (email: Hanan.elabhar@pharma.cu.edu.eg)

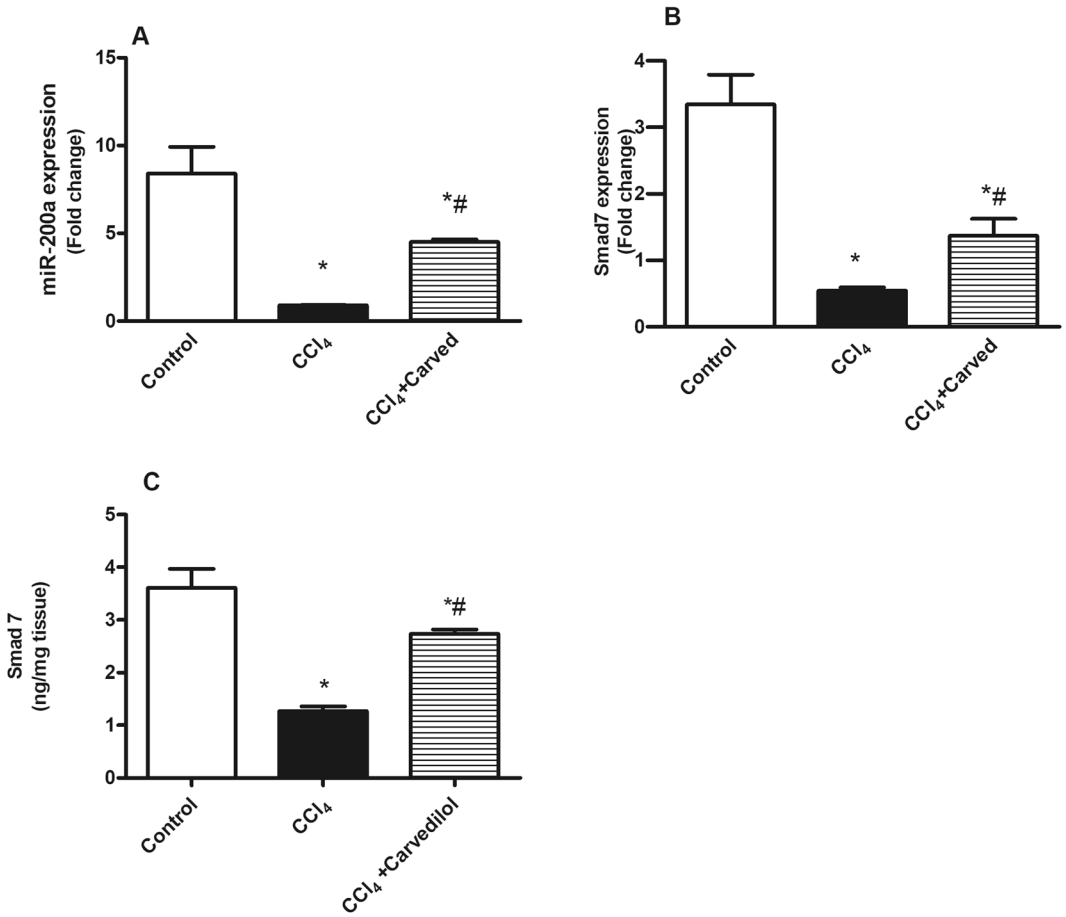

Figure 1. Effect of Carved on gene expression of (**A**) serum miR 200a, and (**B** & **C**) hepatic gene expression/protein content of SMAD7. Values are expressed as mean ± S.D (n = 7). Statistical analysis was carried out using one-way ANOVA followed by Tukey's *post hoc* test, $P < 0.05$. As compared to (*) control group and (#) CCl_4 intoxicated group. Carved treatment (10 mg/kg, p.o, daily) started 2 weeks post CCl_4 (2 ml/kg, i.p) initiation until week 8. Carved: Carvedilol; CCl_4: carbon tetrachloride.

marker TGF-β1 signaling, which is known to wane the epithelial cell adhesion molecule E-Cadherin, and to increase vimentin, a key marker for EMT, and this process was enhanced by the deletion of SMAD7[10,11].

SMAD7 protein is known as the inhibitory SMAD (I-SMAD) or the protective SMAD that switches off signaling of TGF-β1/SMAD, as well as nuclear factor kappa (NF-κB) in liver fibrosis. The latter transcription factor, as well as mitogen activated protein kinase (p38 MAPK) are major cues involved in SMADs signaling[11–13].

Supporting the notion that liver fibrosis is a reversible process, the strategy of emerging anti-fibrotic drugs has been advanced[14]. In 2009, Porter and Turner[15] clarified the correlation between β-blockers and fibrosis; the authors associated the activation of cardiac myofibroblasts to several factors, including hormones as norepinephrine (NE) and highlighted the crucial role of the increased levels of these factors in heart remodeling. Hence, they suggested that certain cardiovascular drugs, including β-blockers, can reduce myocardial remodeling specifically *via* modulatory effects on cardiac fibroblasts[15]. Apart from its antihypertensive effect, Carvedilol, was proven for its anti-fibrotic activity[16–18].

A recent study has associated the myocardial anti-fibrotic role of Carvedilol to a subtype of miRs and SMADs[19]. However, in the liver, the anti-fibrotic mechanism of Carvedilol was explained in terms of its antioxidant and anti-inflammatory properties[16,18,20,21], yet the exact signaling pathways underlying its hepatic anti-fibrotic activity in the context of miR-200a, SMAD7 and EMT are still unknown, which is the aim of this work.

In this study, miR-200a/SMAD7 stream is investigated as one of the pathways contributing to the hepato-protective mechanism of Carvedilol through the suppression of EMT.

Results

Effect of Carvedilol on miR-200a and SMAD7 in CCl_4-induced liver fibrosis. As depicted in Fig. 1, CCl_4 intoxicated group showed a marked downregulation of (A) serum miR-200a gene expression, as compared to the control group. This effect entailed its downstream SMAD7, where the insult decreased its hepatic (B) gene expression and (C) protein content. On the other hand, Carvedilol upregulated serum miR-200a and hepatic SMAD7 by 5 and 2.5 fold, respectively, this effect was reflected also on the protein content of SMAD7 (2.1 folds).

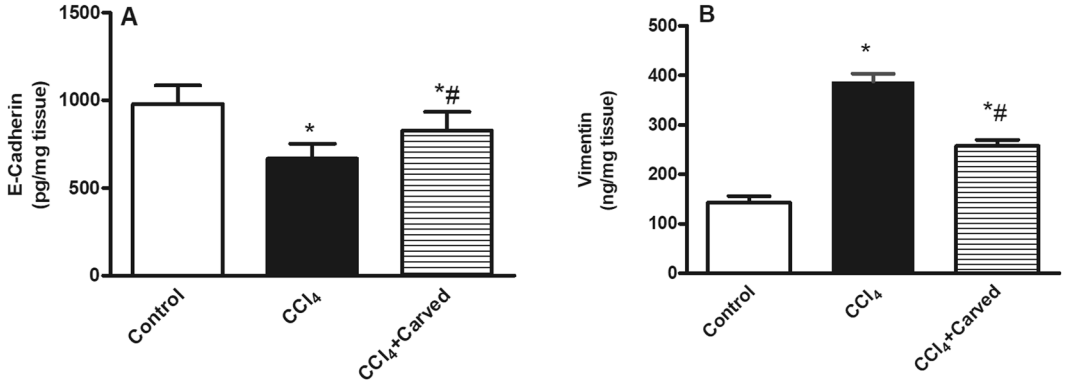

Figure 2. Effect of Carved on hepatic contents of (**A**) E-Cadherin and (**B**) vimentin. Values are expressed as mean ± S.D (n = 7). Statistical analysis was carried out using one-way ANOVA followed by Tukey's *post hoc* test, $P < 0.05$. As compared to (*) control group or (#) CCl_4 intoxicated group. Carved treatment (10 mg/kg, p.o, daily) started 2 weeks post CCl_4 (2 ml/kg, i.p) initiation until week 8. Carved: Carvedilol; CCl_4: carbon tetrachloride.

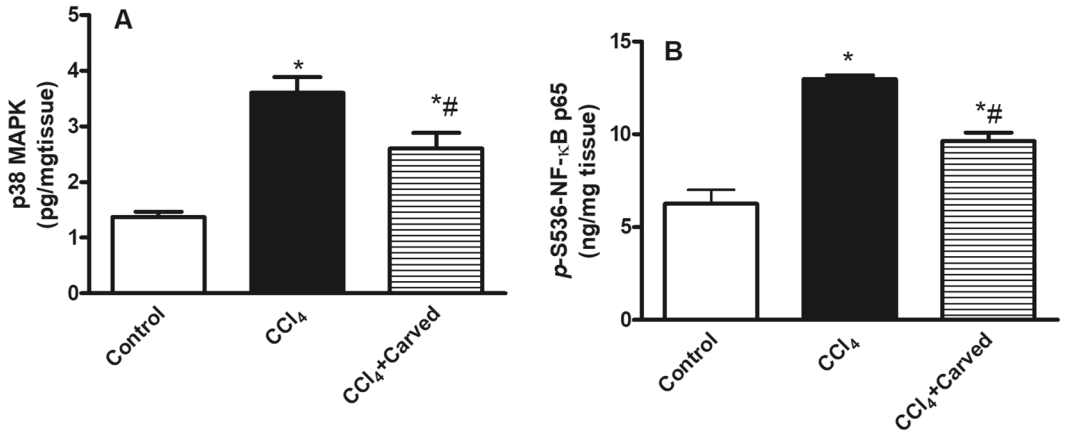

Figure 3. Effect of Carved on hepatic contents of (**A**) p38 MAPK and (**B**) *p*-(S536)NF-κB p65. Values are expressed as mean ± S.D (n = 7). Statistical analysis was carried out using one way ANOVA followed by Tukey's post hoc test, $P < 0.05$. As compared to (*) control group or (#) CCl_4 intoxicated group. Carved treatment (10 mg/kg, p.o, daily) started 2 weeks post CCl_4 (2 ml/kg, i.p) initiation until week 8. Carved: Carvedilol; CCl_4: carbon tetrachloride.

Effect of Carvedilol on hepatic content of mesenchymal to epithelial transition (MET)/epithelial to mesenchymal transition (EMT) markers in CCl_4-induced liver fibrosis. In Fig. 2, CCl_4 reduced the hepatic content of (A) E-Cadherin (668.7+/− 84.67 *vs* normal 979.1+/−106.6), while increased that of (B) vimentin to reach 2.7 folds, as compared to the vehicle group. Carvedilol, however, reverted the CCl_4 effects to raise the MET marker E-Cadherin significantly and to reduce the EMT marker vimentin.

Effect of Carvedilol on hepatic content of inflammatory markers in CCl_4-induced liver fibrosis. The insulted group (Fig. 3) showed a significant increase in the hepatic contents of (A) p38 MAPK and (B) the *p*(S536) NF-κB p65 by 2.7 and 2.1 folds, respectively as compared to the vehicle group. However, Carvedilol counteracted these increments by reducing their levels, respectively by 28% and 26%, as compared to the insulted group.

Effect of Carvedilol on liver function tests in CCl_4-induced liver fibrosis. Figure 4 confirmed the CCl_4-induced liver injury, where in the intoxicated group, the serum levels of (A) ALT, (B) AST, and (C) ALP were elevated by 2.5, 2.7, 3.1 folds, respectively, as compared to the vehicle group, while treatment with Carvedilol has reduced these values significantly. Moreover, (D) the AST to platelet ratio index (APRI) has increased in the insulted group by 3.9 folds relative to the vehicle group, whereas Carvedilol reduced it by 69%, as compared to the CCl_4 intoxicated group.

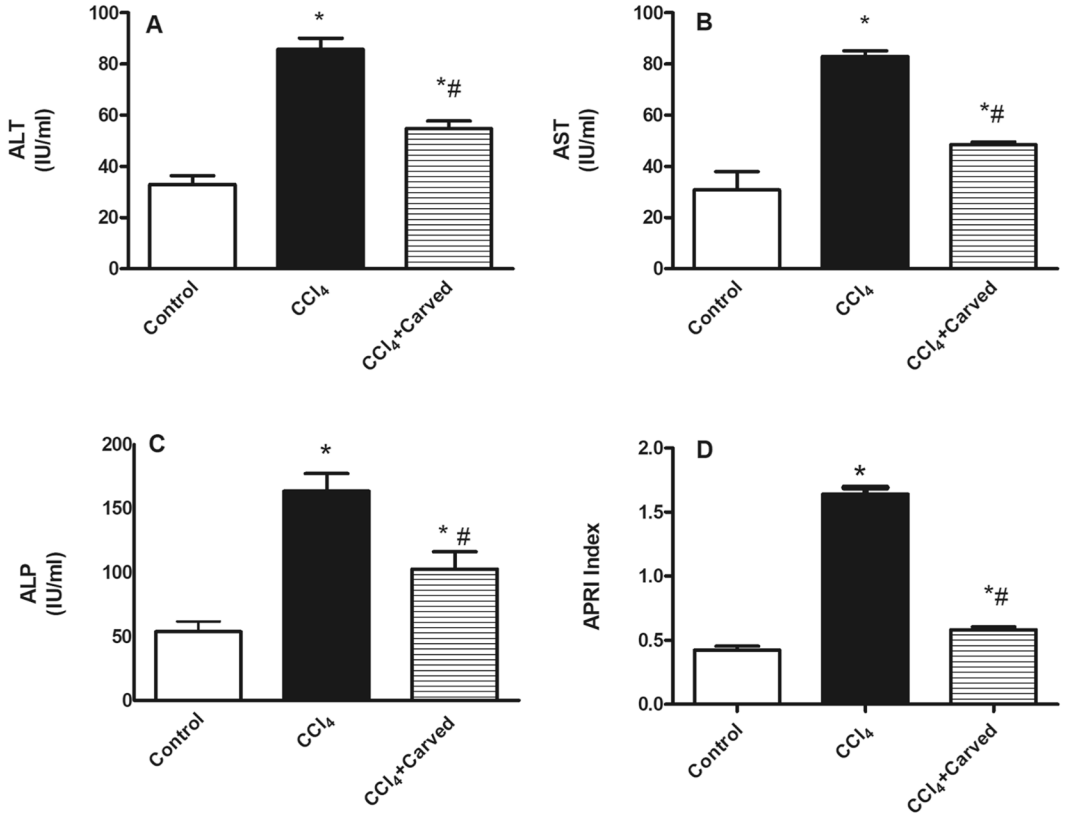

Figure 4. Effect of Carved on liver function tests (**A**) ALT, (**B**) AST, (**C**) ALP and (**D**) APRI. Values are expressed as mean ± S.D (n = 7). Statistical analysis was carried out using one way ANOVA followed by Tukey's *post hoc* test, $P < 0.05$. As compared to (*) control group or (#) CCl_4 intoxicated group. Carved treatment (10 mg/kg, p.o, daily) started 2 weeks post CCl_4 (2 ml/kg, i.p) initiation until week 8. ALP: alkaline phosphatase; ALT: alanine transaminase; AST: aspartate transaminase; APRI: AST/platelet ratio index; Carved: Carvedilol; CCl_4: carbon tetrachloride.

Effect of Carvedilol on immune-histochemical examination of pro-fibrogenic marker/HSC activation markers. As depicted in Fig. 5a, immune-histochemical staining analysis showed that Carvedilol has reduced hepatic expression of the pro-fibrogenic marker TGF-β1 and the marker of HSC activation α-SMA showing minimal brown staining, as compared to the CCl_4 intoxicated group. These results were further confirmed by the percentage area expression of TGF-β1 and α-SMA, as shown in Fig. 5b and c, respectively.

Effect of Carvedilol on liver histopathological changes. Liver photomicrographs (H & E) (Fig. 6) reveal that sections of (C & D) CCl_4 intoxicated group show deposition of collagen fibers in the portal triad [c], vacuolar degeneration of hepatocytes [v], and newly formed bile ductuoles [b], as compared to the (A & B) normal intact histological structure of hepatocytes seen in the vehicle treated sections. Sections of (E & F) Carvedilol treated group reveal improvement in liver structure, where the sections show fine strands of fibroblasts proliferation in the portal triad [f], mild activated Kupffer cells in the portal triad [k], as compared to the CCl_4 intoxicated group. These changes are summarized in panel G according to the Metavir fibrosis scoring.

Effect of Carvedilol on collagen deposition in liver photomicrographs stained with Masson-Trichome stain. In Fig. 7, MTC stain also supported the H & E sections; it shows no histochemical reaction for collagen fibers in the (A & B) normal control group, while sections of (C & D) CCl_4 intoxicated group reveal extensive fibrosis and strong histochemical reaction for collagen fibers in the portal triad and around the hepatic lobules (arrows). On the other hand, sections of (E & F) Carvedilol treated group show weak histochemical reaction of collagen fibers, as compared to the CCl_4 intoxicated group. Panel G shows the changes in area percentage of collagen.

A sum-up of the Carvedilol hepatic anti-fibrotic mechanisms. To recapitulate the current tackled mechanisms/pathways by Carvedilol, Fig. 8 shows that CCl_4 abated miR200-a/SMAD7, as well as E-Cadherin, while enhanced the fibrotic-related markers (vimentin, TGF-β1, α-SMA), as well as the inflammatory markers (p38MAPK, *p*-NF-κBp65) to further augment liver injury. Administration of Carved, however, proved its beneficial effect, as it modulated these pathways significantly in favor of reducing fibrosis.

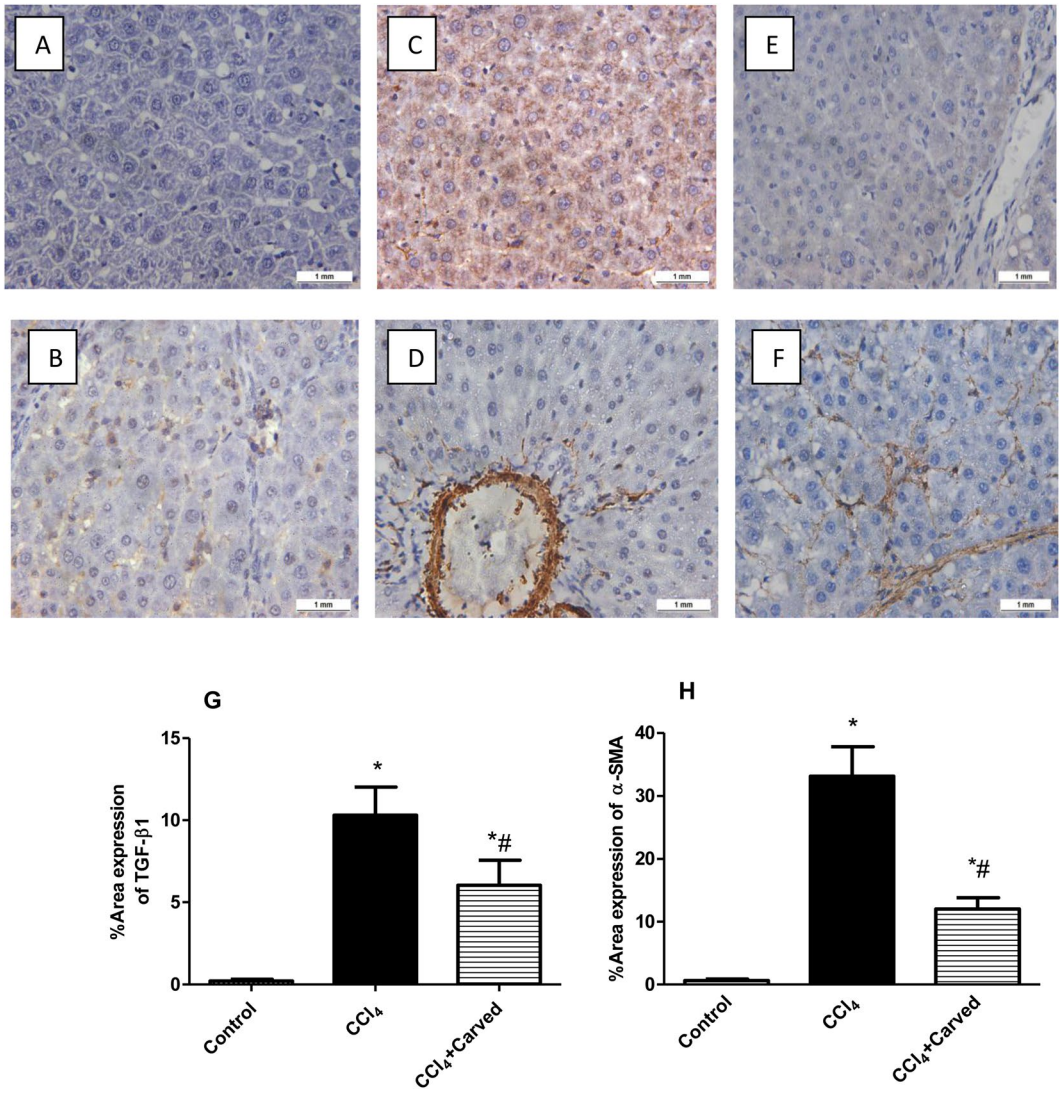

Figure 5. Effect of Carved on immunohistochemical examination of TGF-β1 and α-SMA and their percentage area expression. The immunostained liver cells of normal sections show normal architecture with negative immune-reactivity for (**A**) TGF-β1 and (**B**) α-SMA antibodies. Oppositely, sections from CCl_4 intoxicated group show positive immunoreactivity for (**C**) TGF-β1 and (**D**) α-SMA antibodies (brown discoloration), whereas Carvedilol decreased the immune-reactivity for (**E**) TGF-β1 and (**F**) α-SMA (x100). The percentage area expression of TGF-β1 and α-SMA are shown in panels G and H, respectively. Values are expressed as mean (3 sections/rats/group) ± S.D. Statistical analysis was carried out using one-way ANOVA followed by Tukey's *post hoc* test, $P < 0.05$. As compared to (*) control group or (#) CCL_4 intoxicated group. Carved treatment (10 mg/kg, p.o, daily) started 2 weeks post CCl_4 (2 ml/kg, i.p) initiation until week 8. Carved: Carvedilol; CCl_4: carbon tetrachloride; TGF-β1: transforming growth factor β1; α-SMA: alpha smooth muscle actin.

Discussion

Liver fibrosis is described as a response to chronic injury that can progress to organ failure upon extended damage[22]. This ailment is an endpoint of several factors that assimilate to activate the fibrogenic process. Among these factors is the activity of the sympathetic nervous system, which regulates hepatic fibrogenesis by exerting an effect on hepatic stellate cells[23]. Moreover, Nuamnaichati *et al.* recently described the mechanism of β-blockers in fibrosis revealing that continuous stimulation of the β-adrenergic receptors induces the synthesis and secretion of growth factors in cardiac myocytes that activate cardiac fibroblast, thus, imposing a correlation between these receptors and the activation of fibroblast[24].

Despite this ailment is a historic disease, yet anti-fibrotic therapies are powerless to restrain liver fibrosis in an efficient approach[25]. Nevertheless, Carvedilol, a non-selective β-blocker approved for the treatment of hypertension, has been proven for its efficient hepatic anti-fibrotic properties that are mainly ascribed to its antioxidant and anti-inflammatory properties[16,18,21]. However, in our study, we have evaluated the impact of circulating miR-200a/SMAD7/TGF-β1 axis and the suppression of EMT on the anti-fibrotic effect of Carvedilol.

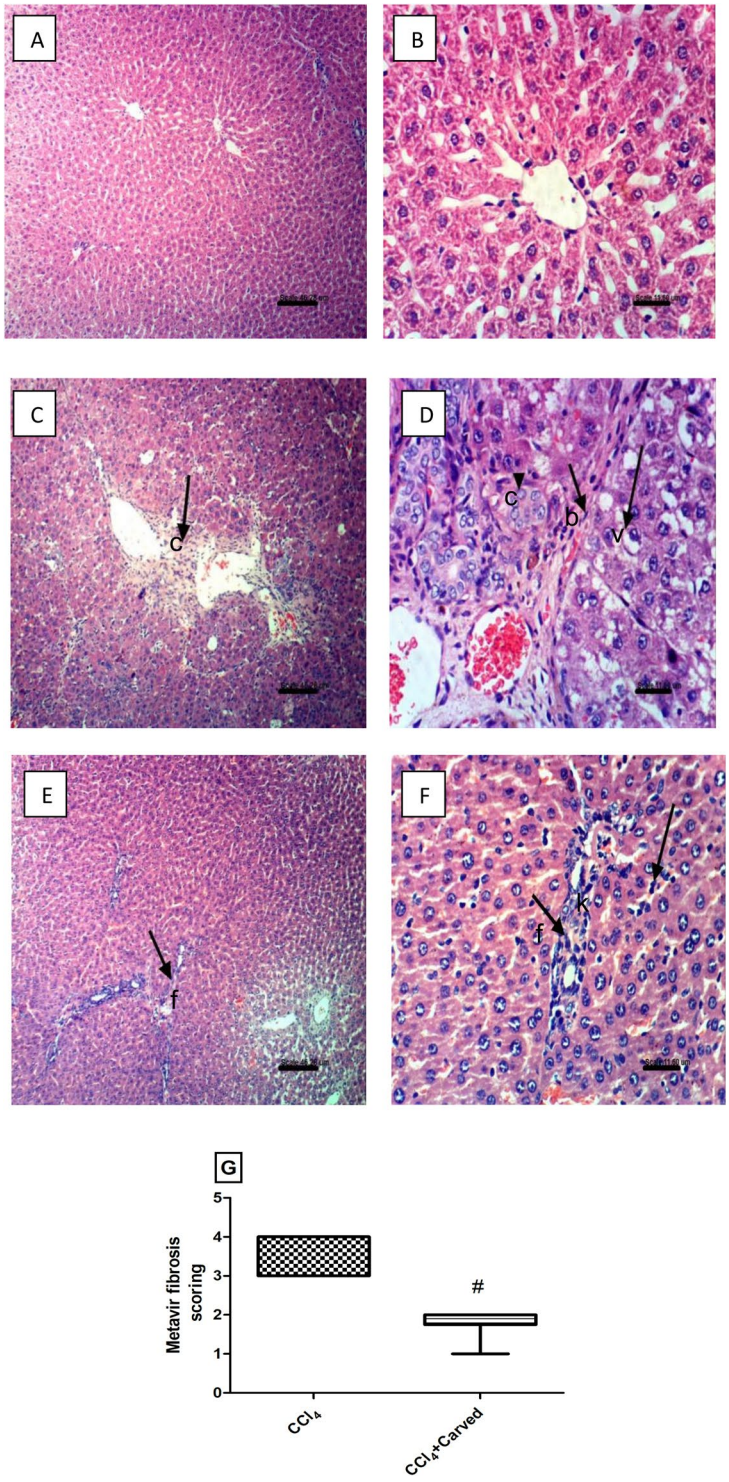

Figure 6. Effect of Carved on photomicrographs of liver sections stained with H&E. Sections of (**C,D**) CCl_4 intoxicated group show collagen fibers deposition in the portal triad [c], vacuolar degeneration of hepatocytes [v], appearance of newly formed bile ductuoles [b] (arrows), as compared to those of (**A,B**) normal group. Sections of (**E,F**) Carved treated group show fine strands of fibroblasts proliferation and instead to prevent repitition [f], Kupffer cells activation and few leucocytes in the portal triad [k] (arrows). (x100; scale bar = 46.2μm; x400; scale bar = 11.6 μm). Panel G reveals METAVIR Fibrosis scoring. Data are expressed as median values (max-min). Statistical analysis was carried out using non-parametric Mann Whitney U test between CCl_4 and CCl_4 + Carved (#), $P < 0.05$. Carved treatment (10 mg/kg, p.o, daily) started 2 weeks post CCl_4 (2 ml/kg, i.p) initiation until week 8. Fibrosis score was evaluated in ten randomly selected fields from each slide. Carved: Carvedilol; CCl_4: carbon tetrachloride.

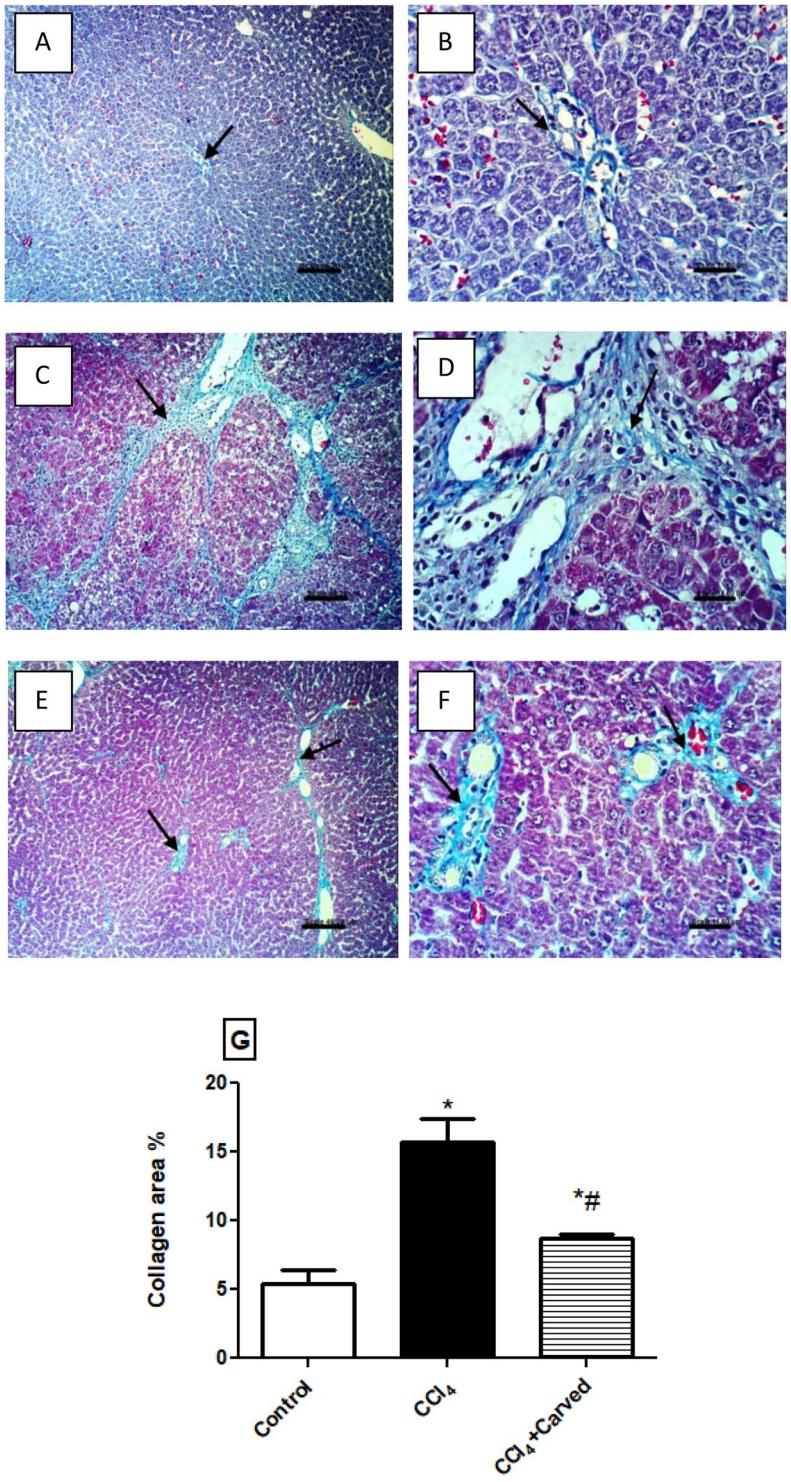

Figure 7. Effect of Carved on photomicrographs of liver tissues stained with Masson Trichome stain. Sections of (**C,D**) CCl_4 intoxicated group show extensive fibrosis and strong histochemical reaction for collagen fibers in the portal triad and around the hepatic lobules (arrows), relative to sections of (**A,B**) normal group showing no histochemical reaction for collagen fibers. Sections of animals treated with (**E,F**) Carved show a weak histochemical reaction for collagen fibers (arrows) (x100, scale bar = 46.2μm; x400: scale bar = 11.6 μm). Panel (**G**) represents percentage area of collagen content in liver tissues. Values are expressed as mean ± S.D (n = 3sections/rat/group). Statistical analysis was carried out using one way ANOVA followed by Tukey's *post hoc* test, $P < 0.05$. As compared to (*) control group or (#) CCl_4 intoxicated group. Carved treatment (10 mg/kg, p.o, daily) started 2 weeks post CCl_4 (2 ml/kg, i.p) initiation until week 8. Carved: Carvedilol; CCl_4: carbon tetrachloride.

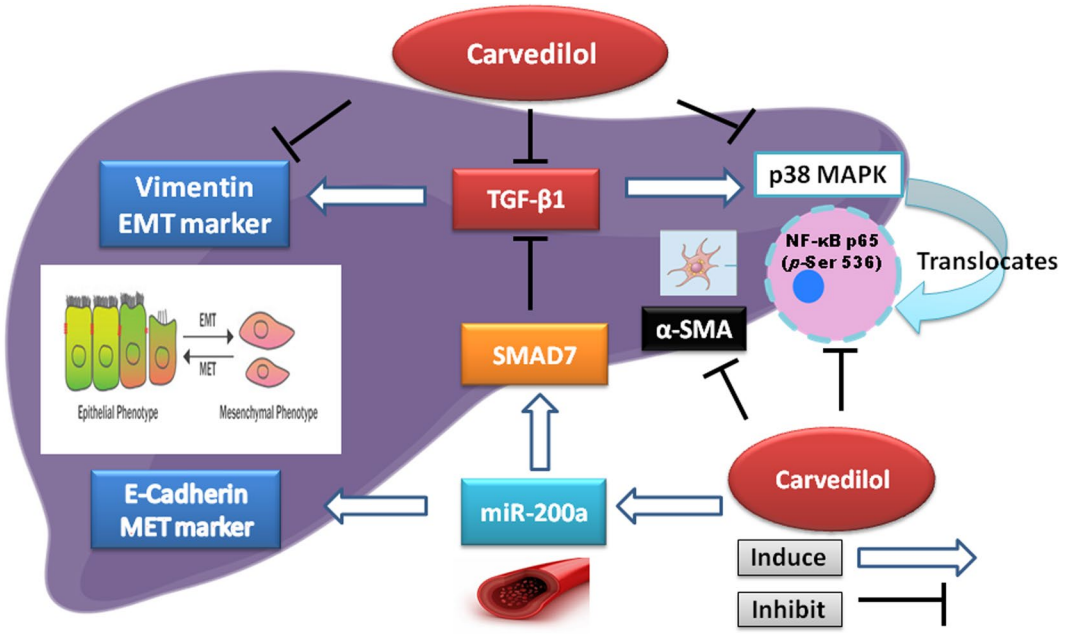

Figure 8. A graphical abstract highlighting the Carvedilol potential mechanism via miR200-a targeting SMAD7/TGF-β1/EMT/MAPK. Carvedilol enhances the gene expression of the circulating anti-fibrotic miR-200a. MiR-200a stimulates the prototypical epithelial marker E-Cadherin, as well as the protective SMAD7, which in return hinders the action of the pro-fibrogenic cytokine TGF-β1. Carvedilol inhibits TGF-β1, the EMT marker α-SMA, *p*-(ser536)NF-κBp65/MAPK and the mesenchymal marker vimentin. MiR-200: microRNA-200a; TGF-β1: transforming growth factor beta 1; EMT: epithelial mesenchymal transition; *p*-(ser536)NF-κBp65: phosphorylated nuclear factor kappa b at serine 536; MAPK: mitogen activated protein kinase.

In this study, Carvedilol significantly upregulated the serum miR-200a gene expression, as compared to the CCl_4 intoxicated group, an effect that is partly responsible for the decreased hepatic fibrosis. In support to our findings, previous studies reported that the expression of miR-200a is downregulated in case of liver fibrosis[26].

Moreover, growing evidence showed that miRNAs participated in hepatic fibrosis through targeting SMAD proteins in liver[27]. SMADs are a group of proteins that mediate the TGF-β signaling and they are targeted by miRNAs[11]. TGF-β is considered as the most powerful commanding pro-fibrogenic cytokine that triggers fibrosis through the enhancement of SMAD-based pathways[28]. This association was further reinforced by a research article revealing that the over expression of miR-200a inhibited SMAD3 activity and attenuated TGF-β1-induced fibrosis[29]; however, the correlation between miR-200a and SMAD7 in liver has not been studied before.

In the current study and in parallel to the miR-200a results, hepatic level of SMAD7 was upregulated in the Carvedilol treated group, as compared to the CCl_4 intoxicated one. This effect was associated with a decrease in the protein expression of TGF-β1, as documented by the current immune-histochemical examination. Our results concur with an earlier study in a model of renal fibrosis[9], where Xiong *et al*. established a correlation between SMAD7 and miR-200 family and they stated that activation of SMAD7 leads finally to hindrance of the TGF-β1-mediated miR-200 downregualtion. Furthermore, a recent study conducted on cardiac fibrosis model, established in human aortic endothelial cells, reported that increased TGF-β1 is responsible for the downregulated expression of miR-200a[30].

A further confirmation for the Carvedilol anti-fibrotic capacity, immunostaining of liver sections with α-SMA antibody divulged a minimal staining of liver tissues in Carvedilol treated group indicating a decline in collagen content, as compared to the CCl_4 intoxicated group, while the latter group showed a brown staining as compared to the vehicle treated group. Similarly, an earlier study confirmed the α-SMA immune-histochemical results[16]. The increased protein expression of α-SMA can be owed to the enhanced TGF-β1, in the current model to match previous findings; Li *et al.*[31] have reported that increased TGF-β1 triggers a rise in α-SMA in a model of renal fibrosis.

EMT is a basic part of liver fibrosis pathology[32]; E-Cadherin and vimentin are classified as type 2 epithelial mesenchymal transition (EMT) markers and this type is responsible for organ fibrosis, wound healing, and tissue regeneration in the liver[33]. In tissue fibrosis, the alteration in E-Cadherin during EMT process is the archetype epithelial marker[34,35]. However, vimentin is a mesenchymal product recognized as type III intermediate filament protein, expressed at the site of injury during the repair phase and declines subsequent to injury resolution[5]. Indeed, E-Cadherin downregulation is mediated through vimentin upregulation to hinder E-cadherin trafficking to the cell[36].The beneficial effect of Carvedilol on miR-200a entailed the modulation of EMT markers, verified by decreasing vimentin and increasing E-Cadherin, as compared to the CCl_4 intoxication. Our findings were in line with Lu *et al*., who revealed that miR-200a hinders EMT *via* the inhibition of vimentin in a pancreatic cancer model[37]. Moreover, parallel studies carried in a model of kidney fibrosis proved that the expression of

miR-200 family obstructed EMT and maintained a high level of E-Cadherin[9]. Additionally, a recent study further supports our results; the authors mentioned in a model of pancreatic fibrosis that TGF-β1 promotes EMT, while miR-200a inhibits it *via* a negative regulation of TGF-β1-induced pancreatic stellate cells activation[38]. It is noteworthy to mention that Gong *et al*. also proved in a recent model of proximal tubules EMT that miR-200a impeded TGF-β1-induced EMT[39]. The reduction of vimentin and the increase of E-Cadherin were enhanced by the upregulation of SMAD7 and the inhibition of TGF-β1.

CCl_4 is a toxin recognized for the induction of liver damage, partially *via* the production of inflammatory cytokines; these cytokines are associated with the activation of mitogen-activated protein kinases (MAPKs) and NF-κB[40]. In normal cells, NF-κB dimer interact with IκBα and produce an inactive complex localized in the cytoplasm. Under stressful conditions, the hepatic cells are activated and this leads to the phosphorylation/degradation of IκBα, which frees activated NF-κB to be translocated into the nucleus[41]. Liver fibrosis pathogenesis is linked to p38 MAPK that phosphorylates and activates the nuclear kinase mitogen- and stress-activated protein kinase (MSK1). In return, activation of MSK1 plays a central role in the activation of NF-κB[42]. Activated p38MAPK can be the missing loop between fibrosis and inflammation, where apart from its fibrogenic role, increased TGF-β1 extends its effect to activate p38MAPK, which in turn stimulates the transcription factor NF-κB. In 2008, Sorrentino *et al*. correlated p38MAPK with the fibrogenic cytokine TGF-β1 after its binding to the TBR1 receptor in a SMAD-independent pathway[43]. This fact should not rule out the role of SMAD7, which when downregulated activates NF-κB p65 through inhibiting IκBα proteins expression to endorse its degradation by phosphorylation[11,44]. These evidences are in agreement with our results, where the hepatic levels of p38MAPK and the active form NF-κB p65 (*p*Ser 536) were significantly raised in CCl_4 intoxicated group, as compared to the normal control group, whereas treatment with Carvedilol significantly diminished them compared to the intoxicated group. We may conclude that the anti-inflammatory capacity of Carvedilol relies on both the inhibition of TGF-β1, as well as the overexpression of SMAD7 to coincide with the results of Wang *et al*. in a renal fibrosis model[44].

The Carvedilol anti-fibrotic effect was mirrored on the improved liver function; as a consequence to the CCl_4-induced hepatic injury, liver enzymes; *viz*., AST, ALT and ALP, were markedly elevated, whereas treatment with Carvedilol leveled them off to signify its hepato-protective effect and to match with a previous study[16]. The ratio of AST to platelet count (APRI) is one of the non-invasive methods used in the assessment and diagnosis of liver fibrosis[45]. In our study, CCl_4 intoxicated group revealed a rise in APRI, however the Carvedilol treated group showed a significant decline in APRI, as compared to the CCl_4 group. Additionally, our results were associated by an improvement in the histopathological examination using H&E and MTC stain, besides the morphometrical collagen quantification test. These examinations revealed collagen deposition and extensive fibrosis detected as karyomegaly of hepatic nuclei and hyperplasia of bile duct in the CCl_4 intoxicated group and this was in agreement with Li *et al*.[46]. On the other hand, Carvedilol improved liver histology and hindered collagen deposition triggered by CCl_4. The significant differences between the intoxicated and Carvedilol groups in fibrosis scoring confirmed the results of the histopathology and morphometry, as Carvedilol has reduced the semi-quantitative fibrosis score in the liver specimens[47]. Our histopathological and morphometrical analysis were in parallel with previous literature[16].

Our results established a recent approach associating the anti-fibrotic mechanism of the non-selective β-blocker Carvedilol with the circulating miR-200a, the newly diagnostic non-invasive biomarkers of liver fibrosis, SMAD7, and through the suppression of EMT.

Materials and Methods

Animals. Thirty adult male Wistar rats (180–200 g) were purchased from National Research Center (Cairo, Egypt). Animals were kept under controlled environmental conditions at a constant temperature (23 ± 2 °C), humidity (60 ± 10%) and a light/dark (12/12 h) cycle at the animal facility of Faculty of Pharmacy, Misr International University (MIU). Food (standard diet pellets; EL-Nasr Co., Abu Zaabal, Egypt) and water were available *ad libitum* until the beginning of the experiment. Animal handling and experimental protocols comply with the Guide for the Care and Use of Laboratory Animals[48], and were approved (PT:1772) by the Research Ethical Committee of the Faculty of Pharmacy, Cairo University (Cairo, Egypt).

Induction of fibrosis and experimental design. Rats were randomly distributed into three groups (10 rats each); animals in group1 received the vehicle dimethyl sulphoxide (1% DMSO), whereas those in group 2 received CCl_4 in olive oil (1:1 v/v) (El Gomhorya Co, Cairo, Egypt; 2 ml/kg; i.p) twice weekly for 8 weeks[49]. Rats in group 3, received CCl_4 as in group 2 and were gavaged Carvedilol (Carvid® MAP S.A.E, Cairo, Egypt) in a dose of 10 mg/kg. Two weeks after initiation of CCl_4, Carvedilol (suspended in 1% DMSO) was administered daily till week 8[16].

Following the termination of experimental protocol, rats were anesthetized with an overdose of thiopental and blood samples were withdrawn from the femoral vein. One aliquot was immediately analyzed manually for platelet count and then confirmed using hemocytometer to be used later for calculating the AST platelet ratio index. Sera were separated from another aliquot and were used for the assessment of liver function tests and circulatory miR-200a. The animals were sacrificed and the liver was harvested and divided into 3 portions. One portion was homogenized in phosphate buffered saline (PBS; 10% w/v), divided into aliquots, and frozen at −80 °C until analysis.

Hepatic content of SMAD7, vimentin, E-Cadherin, p38MAPK and p-S536-NF-κB p65. The rat sandwich ELISA kits were purchased from Life Span BioSciences (Seattle, USA) to assess SMAD7 (cat#LS-F2280) and from MyBiosource (Vancouver, Canada) to assess Vimentin (cat#S032693). Moreover, ELISA kits for

Gene	Forward primer	Reverse primer
miR200a	5′CCTCTGTGGGCATCTTACCG-3′	5′TGGGTCACCTTTGAACATCGT-3′
SMAD7	5′-ACGACTTTTCTCCTCGCCTC-3′	5′TGGACAGTCTGCAGTTGGTTT-3′
β-Actin	5′-GCAGGAGTACGATGAGTCCG-3′	5′ACGCAGCTCAGTAACAGTCC-3′

Table 1. Primers sequence of target genes.

E-Cadherin (cat#ab202413), p38MAPK (cat#ER1138), and *p*-S536-NF-κBp65 (cat#PEL-NFKBP65-S536) were procured from Abcam's ELISA kit (Cambrige, UK), Fine test (Wuhan, Hubei, China), and Ray Biotech (Georgia, USA), respectively. These measurements were performed according to the manufacturer's instructions.

Assessment of hepatic function. Serum aminotransferases (alanine transaminase; ALT, aspartate transaminase; AST) and alkaline phosphatase (ALP) were assessed using the corresponding Stanbio colorimetric assay kits (Liqui-UV; TX, USA).

Histopathological and immune-histochemical examination. Specimens from 3 representative animals/group were fixed in 10% buffered formaldehyde, embedded in paraffin, and sliced with a microtome into 5μm sections. These sections were used for the histopathological and immuno-histochemical examinations. Liver sections were deparaffinised in xylene, washed with ethanol, and placed on glass slides to be stained with Hematoxylin and Eosin (H&E) and Masson trichome (MTC) for histopathological examination of structural changes.

The remaining slices were then immuno-stained with primary antibody anti-TGF-β1 or anti-α-SMA antibody (Santa-Cruz Biotechnology, CA, USA) at a concentration of 1 μg/ml containing 5% BSA (bovine serum albumin) in buffered saline, then incubated with goat anti-rabbit secondary antibody. The percentage expression area of TGF-β1 and α-SMA, as well as liver sections were examined under a light microscope using Leica Quin Plus version 3 (magnification power were x100 x400).

Morphometric analysis and fibrosis scoring. Morphometric analysis of fibrosis was quantified as the mean of 3 consecutive sections/rat/group as a percentage of the total area that was positive for MTC stain in the digital photomicrographs using a computerized image analysis system (Leica Quin plus version 3 software/magnification power x400). The extent of liver fibrosis was evaluated blindly by a pathologist based on METAVIR liver fibrosis scoring system[47]. The scale ranges from 0–4; F0: No fibrosis, F1: Portal fibrosis without septa, F2: Portal fibrosis with few septa, F3: Numerous septa without cirrhosis, and F4: Cirrhosis.

Quantitative real-time PCR for hepatic SMAD7 and serum miR-200a. Total RNA was extracted and purified from serum samples or homogenized liver tissue samples using using miRneasy mini kit including QIAzol Lysis Reagent according to the manufacturer's instructions (Qiagen; Hilden, Germany). For the serum samples, this protocol allows the purification of separate fractions enriched in miR and other small RNA species; for miR recovery a RNeasy MinElute clean up kit was used according to the manufacturer's instructions. SMAD7 and MiR200a gene expression were carried out using gene-specific oligonucleotide primers (Invitrogen, Thermo Fisher Scientific, Inc; CA, USA). Primers sequence for both genes and the housekeeping gene β-actin are presented in Table 1. Total RNA was reverse transcribed to cDNA and amplified in one tube using one-step RT-PCR with SYBR®Green iScript PCR kit (BioRad, CA, USA). Complete reaction mix was incubated in a real time thermal detection cycler as follows: cDNA synthesis at 50 °C for 10 min, reverse transcriptase inactivation 5 min at 95 °C followed by 30 to 45 cycles of amplification 10 s at 95 °C and 30 s at 55 °C to 60 °C. SMAD7 gene expression was carried out using gene-specific oligonucleotide primers (Invitrogen, Thermo Fisher Scientific, Inc; CA, USA). Mean Ct values were used to calculate the relative expression levels of the target gene for the experimental groups, relative to those in the control group. The gene expression data were normalized relative to the housekeeping gene β-actin using the $2^{-\Delta\Delta Ct}$ formula.

Statistical analysis. Parametric data are presented as mean ± S.D (n = 7), all statistical analyses were performed using one-way analysis of variance (ANOVA; $p < 0.05$) followed by Tukey's multiple comparison *post hoc* test. Non-parametric data are presented as box and whiskers with median (max-min) and analysed by Mann-Whitney U test between model and treatment (GraphPad (Prism) software, version 5®).

References

1. Trautwein, C., Friedman, S. L., Schuppan, D. & Pinzani, M. Hepatic fibrosis: Concept to treatment. *J Hepatol* **62**, S15–S24 (2015).
2. Thompson, A. J. & Patel, K. Antifibrotic therapies: will we ever get there? *Curr Gastroenterol Rep.* **12**, 23–29 (2010).
3. Weber, L. W., Boll, M. & Stampfl, A. Hepatotoxicity and mechanism of action of haloalkanes: carbon tetrachloride as a toxicological model. *Crit Rev Toxicol.* **33**, 105–136 (2003).
4. Ogawa, T. *et al.* Suppression of type I collagen production by microRNA-29b in cultured human stellate cells. *Biochem Biophys Res Commun.* **391**, 316–321 (2010).
5. Stone, R. C. *et al.* Epithelial-mesenchymal transition in tissue repair and fibrosis. *Cell and Tissue Research.* **3658**, 495–506 (2016).
6. Bi, W. R., Xu, G. T., Lv, L. X. & Yang, C. Q. The ratio of transforming growth factor-β1/bone morphogenetic protein-7 in the progression of the epithelial-mesenchymal transition contributes to rat liver fibrosis. *Genet. Mol. Res.* **13**(1), 1005–1014 (2014).
7. Zhang, Y. *et al.* Epithelial mesenchymal transition correlates with CD24+CD44+ and CD133+ cells in pancreatic cancer. *Oncol Rep* **27**, 1599–15605 (2012).
8. Murakami, Y. & Kawada, N. MicroRNAs in hepatic pathophysiology. *Hepatol Res.* **47**, 60–69 (2017).

9. Xiong, M. *et al*. The miR-200 family regulates TGF-β1-induced renal tubular epithelial to mesenchymal transition through Smad pathway by targeting ZEB1 and ZEB2 expression. *Am J Physiol Renal Physiol.* **302**, F369–379 (2011).
10. Kalluri, R. & Weinberg, R. A. The basics of epithelial-mesenchymal transition. *J Clin Invest.* **119**, 1420–1428 (2009).
11. Xu, F., Liu, C., Zhou, D. & Zhang, L. TGF-β/SMAD pathway and its regulation in hepatic Fibrosis. *J Histochem Cytochem.* **64**, 157–167 (2016).
12. Kavsak, P. *et al*. Smad7 binds to Smurf 2 to form an E3ubiquitin ligase that targets the TGF beta receptor for degradation. *Mol Cell Biochem.* **6**, 1366–1375 (2000).
13. Zhu, H. J. & Sizeland, A. M. Smad7 differentially regulates transforming growth factor b-mediated signaling pathways. *J Biol Chem* **274** (1999).
14. Schuppan, D. Liver fibrosis: Common mechanisms and antifibrotic therapies. *Clin Res Hepatol Gastroenterol.* **39**, S51–S59 (2015).
15. Porter, K. E. & Turner, N. A. Cardiac fibroblasts: at the heart of myocardial remodeling. *Pharmacol Ther* **123**, 255–278 (2009).
16. Hamdy, N. & El-Demerdash, E. New therapeutic aspect for carvedilol: antifibrotic effects of carvedilol in chronic carbon tetrachloride-induced liver damage. *Toxicol Appl Pharmacol.* **261**, 292–299 (2012).
17. Tripathi, D. & Hayes, P. C. The role of carvedilol in the management of portal hypertension. *Eur J Gastroenterol Hepatol.* **22**, 905–911 (2010).
18. Araújo Júnior, R. F. *et al*. Carvedilol improves inflammatory response, oxidative stress and fibrosis in the alcohol induced liver injury in rats by regulating Kuppfer cells and hepatic stellate cells. *PLoS One.* **11** (2016).
19. Zhu, J. N. *et al*. Smad3 inactivation and MiR-29b upregulation mediate the effect of carvedilol on attenuating the acute myocardium infarction-induced myocardial fibrosis in rat. *PLoS One.* **8**, e75557 (2013).
20. Gao, P., Yang, B., Yu, H. Y., Meng, R. R. & Si, J. Y. Carvedilol alleviates the biliary cirrhosis through inhibiting the endoplasmic reticulum stress. *Eur Rev Med Pharmacol Sci.* **21**, 5813–5820 (2017).
21. Tian, X. *et al*. Carvedilol attenuates the progression of hepatic fibrosis induced by bile duct ligation. *Biomed Res Int.* **2017**, 4612769 (2017).
22. Schuppan, D. & Kim, Y. Evolving therapies for liver fibrosis. *J Clin Invest.* **123**, 1887–1901 (2013).
23. Sigala, B. *et al*. Sympathetic nervous system catecholamines and neuropeptide Y neurotransmitters are upregulated in human NAFLD and modulate the fibrogenic function of hepatic stellate cells. *PLoS One.* **8** (2013).
24. Nuamnaichati, N., Sato, V. H., Moongkarndi, P., Parichatikanond, W. & Mangmool, S. Sustained β-AR stimulation induces synthesis and secretion of growth factors in cardiac myocytes that affect on cardiac fibroblast activation. *Life Sci.* **193**, 257–269 (2018).
25. Wilson, C. L., Mann, D. A. & Borthwick, L. A. Epigenetic reprogramming in liver fibrosis and cancer. *Adv Drug Deliv Rev.* **121**, 124–132 (2017).
26. Sun, X. *et al*. Participation of miR-200a in TGF-β1-mediated hepatic stellate cell activation. *Mol Cell Biochem.* **388**, 11–23 (2014).
27. Murakami, Y. *et al*. The progression of liver fibrosis is related with overexpression of the miR-199 and 200 families. *PLoS One.* **6**, e16081 (2011).
28. Lan, H. Y. & Chung, A. C. TGF-β/Smad signaling in kidney disease. *Semin Nephrol.* **32**, 236–243 (2012).
29. Wang, B. *et al*. miR-200a Prevents renal fibrogenesis through repression of TGF-beta2 expression. *Diabetes* **60**, 280–287 (2011).
30. Zhang, H., Hu, J. & Liu, L. P. MiR-200a modulates TGF-β1-induced endothelial-to-mesenchymal shift via suppression of GRB2 in HAECs. *Biomed Pharmacother.* **95** (2017).
31. Li, Z. *et al*. Pirfenidone suppresses MAPK signaling pathway to reverse epithelial-mesenchymal transition and renal fibrosis. *Nephrology (Carlton).* **22**, 589–597 (2017).
32. Pinzani, M. Pathophysiology of Liver Fibrosis. *Dig Dis.* **33**, 492–497 (2015).
33. Zhao, Y. L., Zhu, R. T. & Sun, Y. L. Epithelial-mesenchymal transition in liver fibrosis (Review). *Biomedical reports.* **4**, 269–274 (2016).
34. Hay, E. D. & Zuk, A. Transformations between epithelium and mesenchyme: normal, pathological and experimentally induced. *Am J Kidney Dis* **26**, 678–690 (1995).
35. Huber, M. A., Kraut, N. & Beug, H. Molecular requirements for epithelial-mesenchymal transition during tumor progression. *Cell Biol* **17**, 548–558 (2005).
36. Mendez, M. G., Kojima, S. & Goldman, R. D. Vimentin induces changes in cell shape, motility, and adhesion during the epithelial to mesenchymal transition. *FASEB J* **24**, 1838–1851 (2010).
37. Lu, Y. *et al*. MiR-200a inhibits epithelial-mesenchymal transition of pancreatic cancer stem cell. *BMC Cancer.* **14** (2014).
38. Xu, M. *et al*. TGF-β1-miR-200a-PTEN induces epithelial-mesenchymal transition and fibrosis of pancreatic stellate cells. *Mol Cell Biochem.* **431**, 161–168 (2017).
39. Gong, Y. *et al*. MicroRNA-200a Inhibits transforming growth factor β1-Induced proximal tubular epithelial-mesenchymal transition by targeting β-Catenin. *Nephron.* **137**, 237–249 (2017).
40. Ma, J. Q., Ding, J., Zhang, L. & Liu, C. M. Ursolic acid protects mouse liver against CCl4-induced oxidative stress and inflammation by the MAPK/NF-κB pathway. *Environ Toxicol Pharmacol.* **37**, 975–983 (2014).
41. Wang, R., Zhang, H., Wang, Y., Song, F. & Yuan, Y. Inhibitory effects of quercetin on the progression of liver fibrosis through the regulation of NF-κB/IκBα, p38 MAPK, and Bcl-2/Bax signaling. *Int Immunopharmacol* **47**, 126–133 (2017).
42. Olson, C. M. *et al*. p38 Mitogen-activated protein kinase controls NF-κB transcriptional activation and tumor necrosis factor alpha production through RelA phosphorylation mediated by mitogen-and stress-activated protein kinase 1 in response to borrelia burgdorferi antigens. *Infect Immun* **75**, 270–277 (2007).
43. Sorrentino, A. *et al*. Isolation and characterization of CD146+ multipotent mesenchymal stromal cells. *Exp Hematol.* **36**, 1035–1046 (2008).
44. Wang, D. T. *et al*. Tanshinone IIA attenuates renal fibrosis and inflammation via altering expression of TGF-β/Smad and NF-κB signaling pathway in 5/6 nephrectomized rats. *Int Immunopharmacol* **26**, 4–12 (2015).
45. Castera, L. & Pinzani, M. Biopsy and non-invasive methods for the diagnosis of liver fibrosis: does it take two to tango? *Gut.* **59**, 861–866 (2010).
46. Li, J. P. *et al*. Nrf2 pathway activation contributes to anti-fibrosis effects of ginsenoside Rg1 in a rat model of alcohol- and CCl4-induced hepatic fibrosis. *Acta Pharmacol Sin.* **35**, 1031–1044 (2014).
47. Bedossa, P. & Poynard, T. An algorithm for the grading of activity in chronic hepatitis C. The METAVIR Cooperative Study Group. *Hepatology* **24** (1996).
48. Iredale, J. Defining therapeutic targets for liver fibrosis: exploiting the biology of inflammation and repair. *Pharmacol Res.* **58**, 129–136 (1996).
49. Iredale, J. P. *et al*. Mechanisms of spontaneous resolution of rat liver fibrosis. Hepatic stellate cell apoptosis and reduced hepatic expression of metalloproteinase inhibitors. *J Clin Invest.* **102**, 538–549 (1998).

Author Contributions

H.S. and S.A. conceived the experimental design. S.A., H.S. and R.M. wrote the main manuscript. S.A. conducted the experiments and analyzed the data. S.A. and H.S. reviewed the main manuscript.

Additional Information

Competing Interests: The authors declare no competing interests.

Publisher's note: Springer Nature remains neutral with regard to jurisdictional claims in published maps and institutional affiliations.